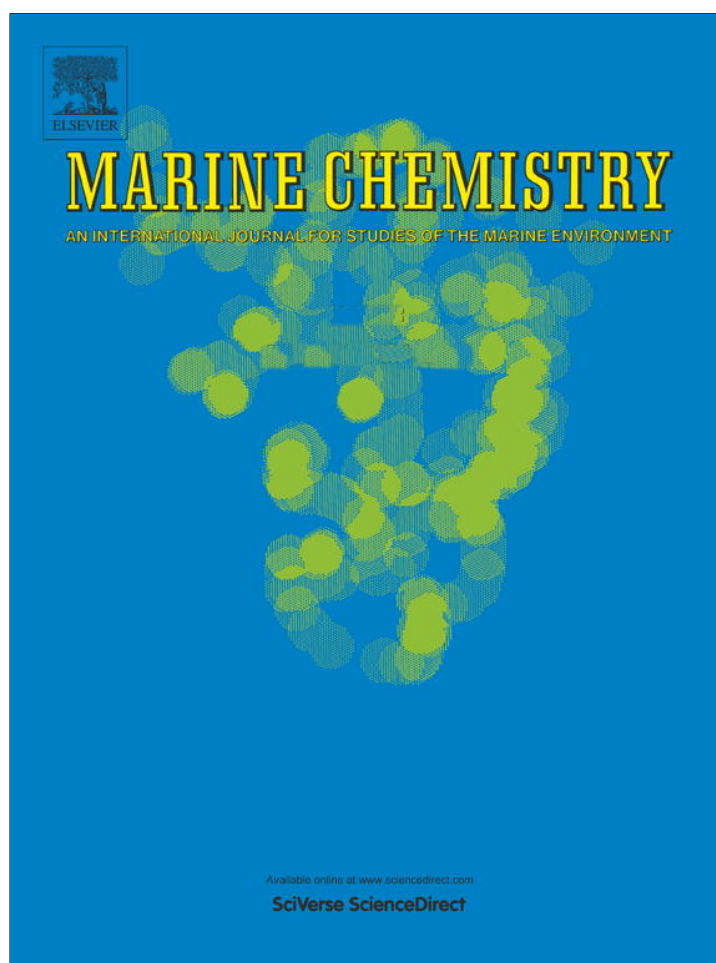


Provided for non-commercial research and education use.
Not for reproduction, distribution or commercial use.



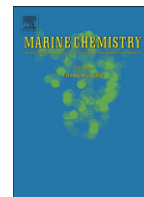
(This is a sample cover image for this issue. The actual cover is not yet available at this time.)

This article appeared in a journal published by Elsevier. The attached copy is furnished to the author for internal non-commercial research and education use, including for instruction at the authors institution and sharing with colleagues.

Other uses, including reproduction and distribution, or selling or licensing copies, or posting to personal, institutional or third party websites are prohibited.

In most cases authors are permitted to post their version of the article (e.g. in Word or Tex form) to their personal website or institutional repository. Authors requiring further information regarding Elsevier's archiving and manuscript policies are encouraged to visit:

<http://www.elsevier.com/copyright>



Changes in compound specific $\delta^{15}\text{N}$ amino acid signatures and D/L ratios in marine dissolved organic matter induced by heterotrophic bacterial reworking

M.L. Calleja*, F. Batista, M. Peacock, R. Kudela, M.D. McCarthy

Department of Ocean Sciences, University of California, 1156 High Street, Santa Cruz, CA 95064, USA

ARTICLE INFO

Article history:

Received 2 July 2012

Received in revised form 3 December 2012

Accepted 4 December 2012

Available online 14 December 2012

Keywords:

Marine dissolved organic matter

Marine dissolved organic nitrogen

Amino acids

Compound specific nitrogen stable isotopes

Bacterial degradation

ABSTRACT

Compound-specific $\delta^{15}\text{N}$ analysis of individual amino acids ($\delta^{15}\text{N}$ -AA) represents a potentially important new tool which may reveal the molecular-level basis for $\delta^{15}\text{N}$ signature of dissolved organic nitrogen (DON) in the ocean, as well indicate DON sources and specific mechanisms of alteration. Past work has indicated that $\delta^{15}\text{N}$ -AA may be effective at indicating the effects of microbial heterotrophy, however the influence of bacterial degradation on $\delta^{15}\text{N}$ -AA patterns has never been directly investigated. Here we measured molecular-level changes in $\delta^{15}\text{N}$ -AA patterns in freshly produced algal high molecular weight (HMW) DON due to heterotrophic bacterial reworking, together with linked changes in enantiomeric (D vs. L) AA ratios and also the AA molar percentage-based degradation index (DI). Our results show a strong increase in degradation with microbial consumption of dissolved organic carbon (DOC), consistent with previous studies. The $\delta^{15}\text{N}$ -AA data show systematically higher $\delta^{15}\text{N}$ values for most individual AA after DOC bacterial reworking, resulting in average increases of 3–6‰ in $\delta^{15}\text{N}$ of total proteinaceous material. The average deviation in the $\delta^{15}\text{N}$ values of all AA (ΣV parameter) also increased with degradation, indicating an increase in $\delta^{15}\text{N}$ -AA pattern complexity, most likely due to selected microbial resynthesis of specific AA. These results show that $\delta^{15}\text{N}$ -AA patterns have the ability to directly track the effects of microbial resynthesis in DON. They indicate that $\delta^{15}\text{N}$ -AA represents a highly specific tracer that provides independent, and yet strongly complimentary, information vs. existing AA-based degradation indicators. Together, our data suggests that heterotrophic microbial degradation in the ocean would be expected to increase $\delta^{15}\text{N}$ values of the oceanic DON pool vs. autotrophic sources. This conclusion is consistent with recent results on $\delta^{15}\text{N}$ signatures of total and HMWDON pool in the open sea, however it also strongly implicates bacterial sources as the likely mechanism for $\delta^{15}\text{N}$ -DON changes. Reevaluating existing DON isotopic data in light of these results may improve our understanding of the influence and mechanism of bacterial reworking on DON long-term preservation in the marine water column.

© 2012 Elsevier B.V. All rights reserved.

1. Introduction

Marine dissolved organic matter (DOM) represents the largest reservoir of reduced carbon and nitrogen in the ocean, where its bioreactive components largely fuel heterotrophic microbial activity. However, the vast majority of ocean DOM, including both dissolved organic carbon (DOC) and dissolved organic nitrogen (DON), is resistant to degradation and acts to sequester carbon and nitrogen from the atmosphere over timescales of decades to millennia (Carlson, 2002; Nagata, 2000). Understanding chemical nature and formation pathways for refractory DON may be particularly important, because it represents by far the largest reservoir of reduced N in the water column, playing a key role in biogeochemical cycling in many oceanic regions (e.g., Berman and Bronk, 2003; Landolfi et al., 2008; Wonga et

al., 2002). The biological inaccessibility of DON that is advected out of surface acts as an important control on upper ocean biological cycles, and its eventual remineralization at depth is a key “N pump,” fundamental to closing oceanic nutrient budgets (Hopkinson and Vallino, 2005; Jackson and Williams, 1985; Williams, 1995). However, despite this significance, the specific sources and molecular transformations which lead to the enormous subsurface refractory DON pool remain largely a mystery.

Heterotrophic bacteria are likely to be key agents in shaping both the amount and composition of DON in the subsurface ocean, where they remineralize about 40% of reduced nitrogen (Andrews and Williams, 1971; Pomeroy, 1974; Suttle et al., 1990). In addition, less well-understood heterotrophic processes may also transform the molecular character of preserved dissolved material. The “microbial carbon pump” (MCP; Jiao et al., 2010) has recently been proposed as unifying framework for a growing consensus that bacterial activity plays a central role in transforming labile components into increasingly refractory DOM. However, and despite extensive research (e.g., Azam and Malfatti, 2007; Mou et al., 2008; Riebesell et al.,

* Corresponding author at: Instituto Andaluz de Ciencias de la Tierra. IACT (CSIC-UGR), Av. de las Palmeras, 4, 18100 Armilla, Granada, Spain. Tel.: +34 958230000x190135; fax: +34 958552620.

E-mail address: marialluch.calleja@gmail.com (M.L. Calleja).

2007; Suttle, 2007), the exact processes which produce this refractory material, and especially which chemical forms can persist in the ocean for millennia, are still not well understood.

The answers about constraints on reactivity are likely to be found in the chemical identity of DOM, coupled with knowledge about biochemical transformations with microbial activity (e.g., Benner, 2002). Isolation and characterization approaches have suggested that, at least at the broad functional level, proteinaceous material may be the dominant DON nitrogen form, in particular in the subsurface ocean (e.g., McCarthy and Bronk, 2008). Amino acids are the major nitrogenous component of DON that can be recovered at the molecular-level at all depths (e.g., McCarthy and Bronk, 2008). They comprise the main ON source from marine plankton (e.g. Hedges et al., 2002; Cowie and Hedges, 1992), and they dominate the sinking particulate organic nitrogen (PON) pool, even when they cannot be recovered at the molecular level via hydrolytic protocols (e.g., Hedges et al., 2001). While it is possible that currently unknown nitrogenous compounds may also contribute, taken together current observations suggest that AA are the single most promising molecular class to study sources, cycling and transformations of the oceanic DON pool.

The central importance of bacteria in DON cycling, coupled with importance of AA in molecular composition, therefore suggests a focus on tracing microbial changes in composition, sources and sinks of proteinaceous material. Molecular-level analysis of AA has long been a powerful approach to investigate organic nitrogen (ON) reactivity. Multiple proxies have been developed to study its character and transformation, including diagenetic maturity indicators from non-protein AA (e.g., Cowie and Hedges, 1994; Wakeham et al., 1997), and also indices of degradation based on mol% composition of individual AA, such as the degradation index (DI, Dauwe et al., 1999; Dauwe and Middelburg, 1998) or the reactivity index (RI, Jennerjahn and Ittekkot, 1997). However mol% patterns typically also have limited source specificity (e.g., Cowie and Hedges, 1992). An additional indicator of DOC source, and possibly diagenetic state, has been enantiomeric (D/L) AA ratios (e.g. Kaiser and Benner, 2008; Pérez et al., 2003). While L-AA dominate the total AA pool and serve as a rapidly cycled substrate for bacterioplankton (Amon et al., 2001), D-AA in ocean DOC are thought to derive mainly from bacterial sources, either from peptidoglycan in cell walls or other natural products (Kaiser and Benner, 2008; McCarthy et al., 1998; Shleifer and Kandler, 1972). D-AA may be also associated with increasingly refractory DOC (Amon et al., 2001; Jørgensen et al., 1999). However, major questions remain regarding specific sources of D-AA, and interpretation of observed D/L ratios with depth (Kaiser and Benner, 2008). A new set of tools permitting a more exact understanding of mechanisms of degradation and/or resynthesis would be key for organic geochemists to identify key mechanisms of DON reactivity and cycling.

Stable carbon ($\delta^{13}\text{C}$) and nitrogen ($\delta^{15}\text{N}$) compound-specific isotope values of individual AAs (CSI-AA) can be used to address some of these challenges, by making isotopic measurements directly on individual AA. In recent years CSI-AA has been rapidly developing as an important new tracer for both source and transformation of nitrogenous material. In particular, $\delta^{15}\text{N}$ CSI-AA patterns ($\delta^{15}\text{N}$ -AA) have been shown to have unique tracer potential to understand food webs, track heterotrophic transformations, and understand the diagenesis of organic nitrogen (e.g., McCarthy et al., 2007; McClelland et al., 2003; Popp et al., 2007; Sherwood et al., 2011). A CSI-AA pattern represents the sum of the isotopic fractionations associated with the biosynthetic pathways in central metabolism for each AA. In heterotrophs and detrital ON, CSI-AA data represents both the autotrophic source signature (e.g. Hayes, 2001; Macko et al., 1986), coupled with any subsequent alteration due to trophic transfers or microbial resynthesis (e.g., Keil and Fogel, 2001; McCarthy et al., 2004). Recent work on $\delta^{13}\text{C}$ signatures of individual AA in DOC has demonstrated the potential of CSI-AA for determining the importance of microbial reworking, and also autotrophic versus heterotrophic

contributions to DOC (McCarthy et al., 2004; Ziegler and Fogel, 2003). McCarthy et al. (2007) further showed that source $\delta^{15}\text{N}$ -AA patterns are generally well preserved in DON and PON, and proposed that microbial alteration to “starting” algal $\delta^{15}\text{N}$ -AA signatures can constitute a broad new index for the extent of microbial AA resynthesis (ΣV parameter). Together, these studies suggest that $\delta^{15}\text{N}$ -AA can provide independent, but highly complementary, information to more traditional AA parameters.

Here we investigate for the first time changes in $\delta^{15}\text{N}$ -AA patterns due to heterotrophic bacterial degradation and reworking in marine DOC. We measured changes in $\delta^{15}\text{N}$ -AA patterns, as well as D/L ratios and DI index, in freshly produced algal HMWDOC with bacterial degradation. A main aim is to develop a more quantitative understanding of heterotrophic $\delta^{15}\text{N}$ -AA signatures for marine DOM, and also to explore specific degradation mechanisms for proteinaceous material. At the same time, these data represent the first direct experiments testing the effects of bacterial degradation on the $\delta^{15}\text{N}$ value of marine DON. Our results show large changes in $\delta^{15}\text{N}$ -AA signatures with ongoing bacterial degradation. Together, our results show that when coupled with traditional AA proxies (AA D/L ratio and DI index), $\delta^{15}\text{N}$ -AA patterns provide unique insight into changes in marine DOC at different stages of microbial degradation. At the same time our results may have important implication for understanding the role of bacterioplankton in shaping $\delta^{15}\text{N}$ value of total DON in the world ocean.

2. Materials and methods

The following methods text refers to Fig. 1, which provides an analytical flow-chart detailing the experimental set-up and progression.

2.1. Phytoplankton cultures growth and harvest

Two *Skeletonema marinoi* cultures were purchased from the Center for Culturing Marine Phytoplankton (CCMP) or the American Type Culture Collection and grown in batch cultures independently in an environmental chamber ($\sim 16^\circ\text{C}$ on a 14/10 light/dark cycle; light levels between $100\text{--}200\ \mu\text{E m}^{-2}\ \text{s}^{-1}$). Cultures grown on filtered artificial f/2 media (Guillard and Ryther, 1962), started in 20 liter volumes and then transferred to a final volume of 200 L in barrels lined with Hyclone gamma-sterilized tank liners, and circulated using filtered bubbled air. While all materials were sterilized or filtered prior to use, in such large cultures it was not possible to maintain axenic conditions. However, the heterotrophic bacterial biomass contribution was measured via flow cytometry, and was always $<1\%$ than total cell biomass. Thus, the organic matter pool isolated from each incubation can be considered phytoplankton-derived. Hereinafter we refer to the two replicate cultures as B1 (barrel 1), and B2 (barrel 2). Algal growth was monitored with fluorescence, and both large cultures were targeted for harvest and processing during exponential growth phase. Growth data however, shows that while B1 was harvested during exponential growth, B2 had already entered senescent conditions at time harvest was initiated (Fig. 2). At harvest, phytoplankton cells (and all bacterial biomass) were removed from the cultures by $0.1\ \mu\text{m}$ hollow-fiber microfiltration (e.g., Roland et al., 2008). A sample of higher molecular weight (HMW) DOC ($>1000\ \text{D}$) was then isolated by tangential flow ultrafiltration (UF; see below) from 40 liters of culture. This “fresh” plankton-derived HMW-DOC sample represented the starting material for bacterial degradations.

2.2. Bacterial-DOC incubations and DOC sampling

The remaining 160 liters of DOC isolated from each phytoplankton culture was then inoculated with pre-filtered surface seawater ($0.6\ \mu\text{m}$ cartridges; opticap XL5 by Millipore) from the central Californian coast (36.9°N , 122.1°W) at a 4% dilution. Both incubations were conducted

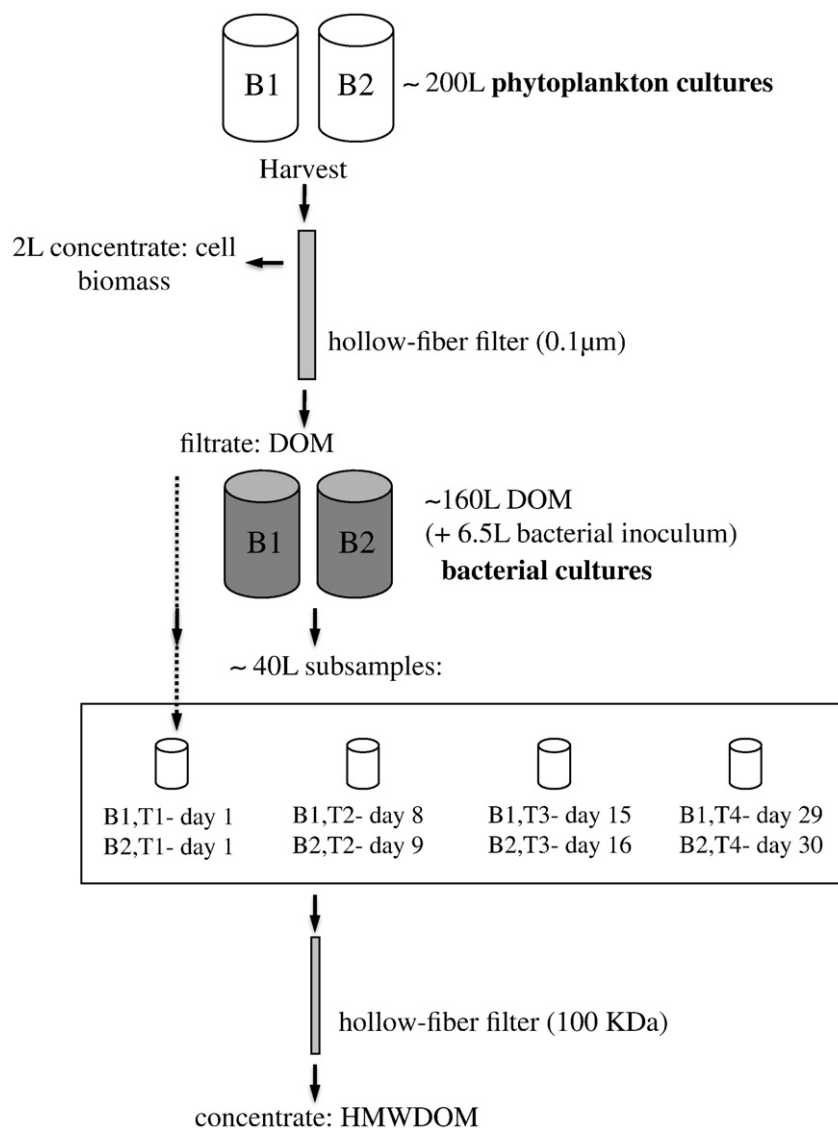


Fig. 1. Diagram showing the experimental set up and sampling methodology.

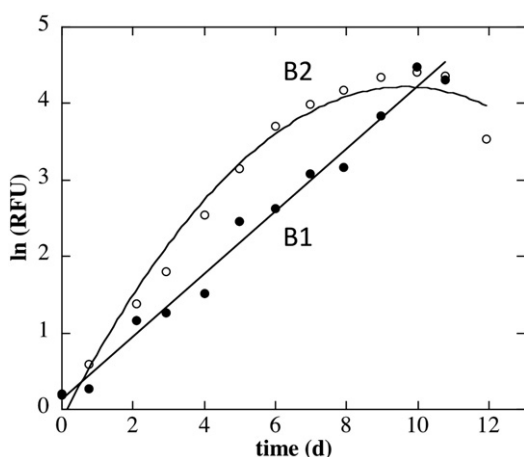


Fig. 2. Growth curves for *Skeletonema marinoi* cultures, expressed as change of relative fluorescence units (RFU) with time in days (d) in the replicate large volume cultures Barrel 1 (B1, full circles) and barrel 2 (B2, empty circles). The last point in each line represents the time when cultures were harvested. Solid lines represent fitted regressions: for B1 linear regression $\ln(\text{RFU}) = 0.13 (\pm 0.11) + 0.41 (\pm 0.02) t(\text{d})$; $r^2 = 0.98$, $P < 0.0001$; for B2 polynomial curve function $\ln(\text{RFU}) = -0.12 (\pm 0.11) + 0.90 (\pm 0.01) t(\text{d}) - 0.05 (\pm 0.004) \times t^2(\text{d})$; $r^2 = 0.99$, $P < 0.0001$.

in the dark at 15°C for 30 days. Subsamples for DOC concentrations (reported in $\mu\text{mol C L}^{-1}$) and for bacterial abundance (BA) (reported as cell ml^{-1}) were taken daily during the first two weeks, and every two days during the following weeks of incubation.

Subsamples for HMWDOC were isolated from cultures after 8, 15 and 29 days in barrel 1, and after 9, 16 and 30 days of bacterial incubation in barrel 2. A 100 kDa hollow-fiber microfiltration membrane was first used to remove bacterial biomass, and then HMWDOC (> 1 kDa) was isolated following standard protocols (e.g., Benner et al., 1997; McCarthy et al., 2007). Briefly, HMWDOC samples were isolated using a spiral-wound 1 kDa polysulfone membrane (SOC 1812 cartridge, Separation Engineering Inc.). Salts were removed from ultrafiltration concentrates by diafiltration with 15–20 L of MQ water. Desalted concentrates were frozen immediately after collection, dried in a Savant Speed-Vac evaporator and pelleted for lyophilization and hydrolysis.

2.3. Chemical and isotopic analysis

2.3.1. DOC and HMW-DOC concentration analysis

20 ml of 100 kDa and 1 kDa filtered water were transferred to pre-combusted glass ampoules (450 C for 5 h) and kept acidified (pH: 1–2) until analysis by High Temperature Catalytic Oxidation on a Shimadzu

TOC-VCPH (Benner and Strom, 1993; Sharp et al., 2002). Every day instrument and water blanks, together with a calibration curve based on variable concentrations potassium hydrogen phthalate, were performed to account for analytical blanks during DOC analyses. Community DOC reference standards (44–45 $\mu\text{mol C L}^{-1}$ and 2 $\mu\text{mol C L}^{-1}$), provided by D. A. Hansell and Wenhao Chen (Univ. of Miami), were used to monitor the ultimate accuracy of DOC concentration data.

2.3.2. Ammonium (NH_4) concentration analysis

20 ml of 100 kDa filtered culture water were transferred to disposable polyethylene centrifuge tubes and kept frozen until analysis on a Technicon AutoAnalyzer II (Solórzano, 1969).

2.3.3. Bacterial abundance and biomass

Bacterial abundance was determined by flow cytometry, with all materials sterilized prior to use. Samples taken from the cultures (1.6 ml) were preserved with 1% paraformaldehyde (final concentration), let stand for 15 min in the dark, then flash frozen in liquid nitrogen and stored at -80°C . Prior to analysis, the samples were thawed, stained with Syto13 (Molecular probes) at 2.5 μM (diluted in DMSO). After standing in the dark for a few min, bacteria were enumerated on a Becton and Dickinson FACSCalibur cytometer. Bacterial biomass was estimated from bacterial abundance assuming a conservative conversion factor of 20 fg C cell $^{-1}$ (Lee and Fuhrman, 1997).

2.3.4. Bacterial growth efficiency (BGE) and CO_2 yield

BGE was estimated as the ratio of bacterial production rate ($\mu\text{mol C L}^{-1} \text{d}^{-1}$ increase in bacterial biomass; ΔBB), to the consumption of available carbon ($\mu\text{mol C L}^{-1} \text{d}^{-1}$), which in turn was estimated from the decrease in total DOC (ΔDOC). Therefore BGE (%) was calculated as $[\Delta\text{BB}/(-\Delta\text{DOC}) \times 100]$. Bacterial C production rates were estimated from the increase in cell number using a conservative C/cell factor of 20 fg C cell $^{-1}$ (Lee and Fuhrman, 1997). Carbon utilization rates were estimated from the decrease of DOC concentrations throughout the incubation. We assume that the remainder of the C balance (100%–BGE) corresponds to respiration, and results in metabolic CO_2 release into the ambient medium, which we call here the CO_2 yield.

2.3.5. Total hydrolyzable amino acid (THAA) and D/L ratios

The total hydrolyzable amino acid (THAA) and enantiomeric measurements were performed following hydrolysis for individual AA using trifluoroacetyl/isopropyl ester (TFA) derivatives, following previously published procedures (McCarthy et al., 2007; Silfer et al., 1991). Briefly, lyophilized HMWDOM samples were hydrolyzed (6 N HCl) for 20 h at 110°C . Samples were evaporated to dryness under a stream of N_2 , and stored in a vacuum desiccator overnight. Individual AA were then converted to TFA derivatives according to a modified protocol after Silfer et al. (1991). After derivatization individual D- and L-amino acid concentrations and molar percentage (mol%) were first measured via gas chromatography coupled to mass spectrometry (GC–MS) on a high sensitivity Agilent 5975B System, fitted with a chiral column (Varian Chrasil-Val, 25 m, 0.25 mm ID). D/L ratios were measured for alanine (Ala), isoleucine (Ile), leucine (Leu), methionine (Met) and phenylalanine (Phe) and mol% in each sample was measured for the same AAs plus glycine (Gly), serine (Ser), valine (Val), proline (Pro), and Tyrosine (Tyr). Asparagine and glutamine are deaminated during acid hydrolysis protocols, and so are quantified as combined peaks: aspartic acid + Asparagine (Asx) and glutamic acid + glutamine (Glx). Acid hydrolysis can also induce racemization of amino acids (e.g., Frank et al., 1979; Kaiser and Benner, 2005; Liardon et al., 1981), which can result in overestimation of D-enantiomers. To correct for hydrolysis-induced racemization we applied the correction equations proposed by Kaiser and Benner (2005), determined for the same hydrolysis conditions. THAA, amino acid mol % and enantiomeric data is shown in Table 1.

2.3.6. Compound specific isotopic amino acid analysis

$\delta^{15}\text{N}$ values were subsequently measured within one week on the same TFA derivatives using a Thermo Trace gas chromatograph (fitted with a Agilent DB-5 column; 50 m, 0.5 mm ID; 0.25 μm film) coupled to a Finnegan Delta-Plus isotope ratio mass spectrometer (GC–IRMS). The minimum total mass required to measure $\delta^{15}\text{N}$ values for the full suite of recoverable individual amino acids under our analytical setup was ~ 450 mg of HMWDOM isolate. For each HMWDOM derivative sample 5 replicate injections were made, with an associated averaged standard error of 1.1‰ across all amino acids measured. Under our analytical conditions $\delta^{15}\text{N}$ values were determined for the following AA: Ala, Asx, Glx, Ile, Leu, Val, Gly, Ser, Met and Phe. Accurate $\delta^{15}\text{N}$ values for Met and Phe were not possible due to low concentrations in several samples. Val, Pro and Tyr were chromatographically separated, however these AA are not reported because either small peak size and/or co-elution precluded accurate $\delta^{15}\text{N}$ value determination in most samples; their inclusion would therefore make direct inter-comparison between samples impossible. Isotopic data is shown in Table 2.

In our data presentation, we have ordered our AA isotopic results according into the two groups (Trophic vs. Source AA) most commonly used in the CSI-AA marine literature. The “Trophic” AA group (Tr-AA; Glx, Asx, Ala, Ileu, Leu and Val) are those which have strongly elevated $\delta^{15}\text{N}$ values with each trophic transfer in animals, while the “source” group (Gly, Ser, Met, Phe, sometimes Thr) have been observed to have $\delta^{15}\text{N}$ values which change little with trophic transfer, at least for planktonic ecosystems (e.g., Chikaraishi et al., 2009; McCarthy et al., 2007; McClelland and Montoya, 2002; Popp et al., 2007). While the trophic vs. source designation is not likely to be directly relevant to microbial degradation, we have followed this convention to make our data presentation directly comparable to most extant literature.

2.3.7. $\delta^{15}\text{N}$ -AA parameter, ΣV

The ΣV parameter, a proxy for total heterotrophic resynthesis proposed by McCarthy et al. (2007), is based on the variance of absolute $\delta^{15}\text{N}$ -AA values around the mean. This parameter therefore also inherently functions as a normalization, expressing only changes to the relative $\delta^{15}\text{N}$ -AA pattern, but eliminating inter-sample variation proposed by McCarthy et al. (2007). We calculated ΣV using all commonly measured AA from our data set. ΣV therefore represents the average deviation (e.g., Bevington and Robinson, 2003) in the $\delta^{15}\text{N}$ values:

$$\Sigma\text{V} = \frac{1}{n} \sum \text{Abs}(\chi_i) \quad (1)$$

where χ_i is the deviation in $\delta^{15}\text{N}$ of each AA i from the average = $[\delta^{15}\text{N}_i - \text{AVG } \delta^{15}\text{N}_i]$, and n is the total number of AA used in the calculation. Using the overall average reproducibility for HMWDOM analysis across our data set (± 1.1 ‰), the average propagated standard analytical error for the ΣV calculation is ± 0.4 ‰.

2.3.8. DI index

The degradation index (DI), proposed by Dauwe and Middelburg (1998), was calculated using all the mol% amino acid composition measured in each HMWDOM sample. DI was determined according to the formula proposed by Dauwe et al. (1999):

$$\text{DI} = \sum_i \left[\frac{\text{var}_i - \text{AVG var}_i}{\text{STD var}_i} \right] \times \text{fac.coef}_i \quad (2)$$

where DI is the degradation index, var_i is the mol percentage of amino acid i , AVG var_i and STD var_i are its mean and standard deviation in our data set, and fac.coef_i the factor coefficient for amino acid i based on the first axis from Table 1 in Dauwe et al. (1999).

2.4. Terminology

Our main focus is to examine $\delta^{15}\text{N}$ -AA changes in DON pool with bacterial degradation, and specifically heterotrophic bacterial change in CSI-AA patterns. "Degradation," however, is a broad concept, which includes a range of mechanistic processes. These include remineralization, selective removal of more labile biochemicals, and also possibly the incorporation of new molecules, either re-synthesized by bacteria, or from de-novo bacterial synthesis. Throughout the manuscript we therefore use "resynthesis" to indicate the heterotrophic synthesis of AA, i.e. AA incorporated into new heterotrophic biomass. This term differs from the "de novo synthesis" in that the latter would also include AA synthesis occurring in autotrophs from mineral C and N sources. We refer to "salvage incorporation" to indicate the uptake and incorporation of existing AA into bacterial biomass with both the C skeleton and all N atoms unchanged. Finally, we use the term "remnant material" to denote macromolecular proteinaceous material (or biomass) that has not been hydrolyzed, and thus has survived heterotrophy with its primary AA structure and original isotopic signatures intact. Distinguishing the relative importance of these fundamental individual processes is necessary to understand the mechanistic basis for CSI-AA changes.

3. Results and discussion

3.1. Phytoplankton DOC sources

The growth curves of *S. marinoi* cultures at time of harvest (the last time point of each curve in Fig. 2), indicated that despite the initial goal of replicate cultures, the algal DOC source character was likely different for B1 vs. B2. The B1 growth curve is strongly linear ($r^2=0.98$, $P<0.0001$), indicating that algal DOC harvested from B1 represents diatom exudates derived from exponential growth. In contrast, while B2 was grown under identical conditions and time frame, it was not possible to harvest the cells and DOC until day 12. The growth curve by this time is clearly non-linear (polynomial curve fit $r^2=0.99$, $P<0.0001$). This suggests beginning of senescence, such DOC composition in B2 may have been influenced by differing DOM exudate compositions (Biddanda and Benner, 1997; Biersmith and Benner, 1998), or contributions from cytosol material from deterioration and breakdown of phytoplankton cells.

DOC concentrations at the time of harvest (corresponding to the initial conditions of bacterial incubations) did not show significant differences within the two cultures, averaging $160 \pm 1.4 \mu\text{mol C L}^{-1}$. However, the relative contribution of HMWDOC in the DOC of B2 was almost double ($27 \mu\text{mol C L}^{-1}$, 17% of DOC) than that in B1 ($14 \mu\text{mol C L}^{-1}$, 9% of DOC). The increased contribution of HMWDOC from the senescent diatoms could be due to increased excretion of HMW carbohydrate-rich material (Biddanda and Benner, 1997), however the strongly increased THAA concentrations in B2 (2926 nmol L^{-1}) vs. B1 (1701 nmol L^{-1}) also suggests the release of protein-rich HMW cytosol material associated with cell death and lysis. The C normalized yields (% C yield) of THAA (% of organic carbon as AAs) are also a very good indicator for microbial degradation of algal-derived amino acids

(Davis et al. 2009). In this study the calculated C normalized yields of THAA at the HMWDOC fraction were significantly higher in B1 (11.2%) vs. B2 (8.5%), consistent with B2 HMWDOC material having already undergone some bacterial biodegradation. Accordingly, bacterial abundances in the two cultures at harvest were also very different: total bacterial cells in B2 ($5.03 \times 10^6 \text{ cells ml}^{-1}$) were approximately an order of magnitude greater than those in B1 ($5.82 \times 10^5 \text{ cells ml}^{-1}$). These observations suggest that DOC starting material for microbial degradation experiments in B2 may have already undergone significant heterotrophic degradation. Together, these observations indicate that both the composition, and likely the degradation state, of DOC used for further microbial incubations were quite different for B1 vs. B2. While not our initial intention, this diversity DOC source character likely strengthens the structure of our experiment, and allows us to compare two different bacterial degradation scenarios that encompass wider and more realistic scenario for heterotrophic degradation $\delta^{15}\text{N}$ -AA patterns in the real ocean.

3.2. Bacterial-DOC incubations

3.2.1. Change in DOC concentration and bacterial abundance

Fig. 3 shows the evolution of concentrations of DOC, HMWDOC and bacterial abundance in incubations during first 16 days, which was the period in which HMWDOC remained abundant enough to quantify AA isotopic values. Initial DOC concentrations (day 0) are those present at phytoplankton culture harvest discussed above. Bacterial abundances are those generated by growth after seawater inoculation; since the same 4% volume inoculation was used for each barrel, initial bacterial abundances were therefore identical (4.3×10^4). Note again that these bacterial abundance estimates are not to be confused with those discussed above (at the end of the phytoplankton culture), since all bacterial biomass in cultures was removed at harvest by the protocol for HMWDOC isolation.

General degradation patterns were similar in both barrels, with maximum bacterial growth rates occurring during the first week of incubation, reaching maximum bacterial abundance of 3.93×10^6 in B1 and 2.6×10^6 in B2. Both DOC and HMWDOC decreased with time, also reaching very similar final values in both barrels, averaging 133 ± 2 and $6.1 \pm 0.4 \mu\text{mol C L}^{-1}$ for DOC and HMWDOC respectively. Bacterial utilization rates, however, were always greater for the HMW fraction (2.2 and $2.7\% \text{ d}^{-1}$ for B1 and B2 respectively) than for the total DOC (1.7 and $2.5\% \text{ d}^{-1}$ for B1 and B2 respectively). These rate differences with MW are consistent with size-reactivity continuum ideas proposed by Amon and Benner (1996), suggesting that algal-derived HMW material present in both barrels at the start of degradations was more labile than total DOC.

Differences in the growth rates, carbon consumption, and growth efficiency between the two barrels are also all consistent with the quality of starting DOC being different in the two experiments. However, a comparison of specific values between barrels paints a more complex picture of DOC quality. The calculated bacterial growth efficiency was much higher in B1 (60%) than in B2 (18%), similar to the higher end of BGE reported for marine coastal waters (e.g., del Giorgio

Table 1
Concentration of total hydrolyzable amino acids (THAA, nmol L^{-1}), amino acid molar percentage (mol%), and D/L ratios of those AA with major D contributions. B1 and B2 refer to barrel 1 and barrel 2 respectively, at the three incubation time points (T1, T2, T3) described in text for which HMWDOM was harvested. AA abbreviations are as defined in the Materials and methods.

Experiment	Time (d)	THAA (nmol L^{-1})	Trophic AA										Source AA								
			Glx		Asx		Ala		Ile		Leu		Pro	Val	Met		Phe		Gly	Ser	Tyr
			mol%	D/L	mol%	D/L	mol%	D/L	mol%	D/L	mol%	D/L	mol%	mol%	mol%	D/L	mol%	D/L	mol%	mol%	mol%
B1 T1	1	1531	7.5	0.00	20.1	0.05	20.1	0.03	3.2	0.01	8.8	0.13	n.d.	19.6	0.8	0.07	2.6	0.03	10.2	6.2	0.03
B1 T2	8	1362	0.2	0.04	5.5	0.12	39.0	0.06	3.9	0.06	14.4	0.22	1.1	15.0	0.0	0.15	0.2	n.d.	11.7	8.1	0.02
B1 T3	15	44	0.3	1.15	4.7	0.96	2.9	0.09	3.8	0.08	2.6	0.23	0.1	2.0	2.6	0.15	n.d.	n.d.	19.7	60.8	0.08
B2 T1	1	2274	3.7	0.00	12.6	0.05	25.6	0.00	2.8	0.03	6.0	0.15	0.3	12.6	0.9	0.01	4.4	0.02	13.9	17.0	0.02
B2 T2	9	1922	5.4	0.06	19.2	0.63	27.4	0.01	4.0	0.02	8.1	0.16	0.8	18.0	0.1	0.15	n.d.	n.d.	14.9	2.1	0.02
B2 T3	16	3	3.8	0.27	24.7	4.16	3.3	0.10	4.7	0.44	20.6	5.48	9.8	n.d.	9.3	0.68	n.d.	n.d.	14.1	4.6	5.23

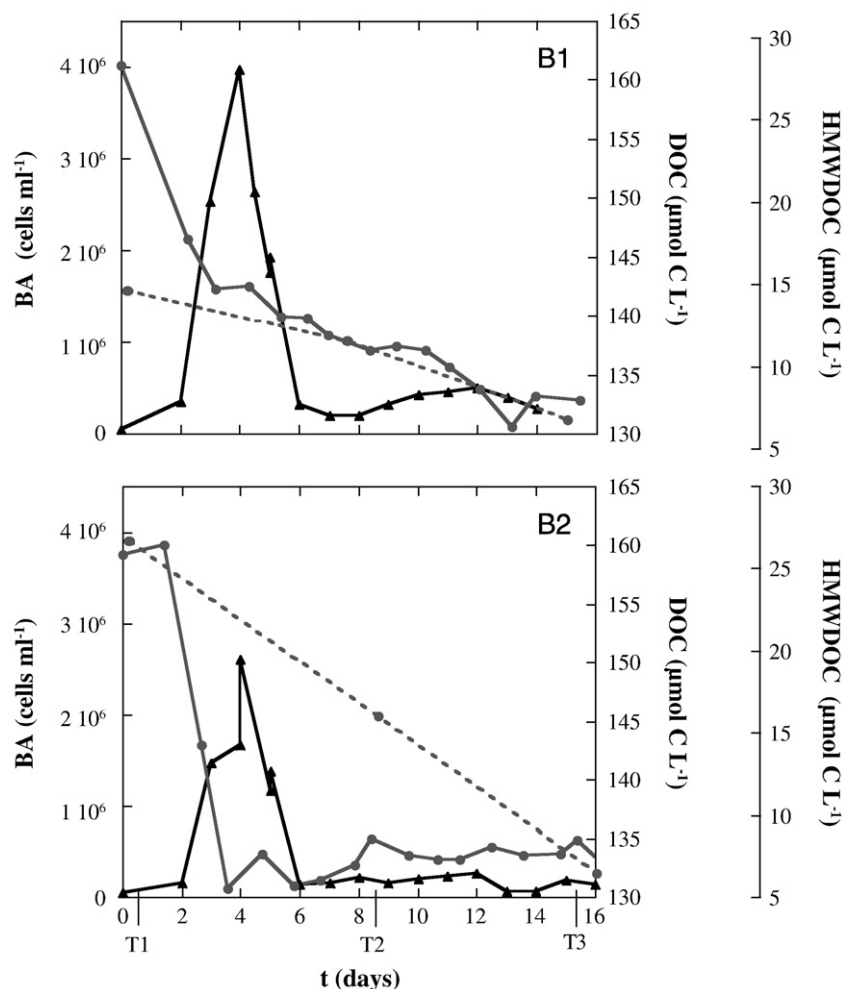


Fig. 3. The relationship of bacterial abundance (BA, in cell ml^{-1} ; black triangles with solid line), dissolved organic matter concentration (DOM, in $\mu\text{mol C L}^{-1}$; gray circles with solid line), and high molecular weight dissolved organic matter concentration (HMWDOC, in $\mu\text{mol C L}^{-1}$; gray circles with dashed line), vs. time (days) during the bacterial incubations. Upper panel: barrel 1 (B1); Lower panel, barrel 2 (B2). T1, T2 and T3 represent the time points where HMWDOC fraction was isolated for further molecular-level and isotopic AA analysis.

and Cole, 1998). These higher values are consistent with the idea that DOC in B1 was “fresher,” and therefore could be more efficiently incorporated into bacterial biomass, vs. B2. However, carbon consumption rates for DOC, were significantly higher in B2 ($2.5\% \text{ d}^{-1}$) than in B1 ($1.7\% \text{ d}^{-1}$) (differences are outside the propagated error for daily consumption rates), suggesting that some aspects of DOC character appear to be more labile when derived from the senescent DOC vs. the fresh exudates. This observation is also consistent with the higher concentrations of both, HMWDOC and THAA, found in B2 vs. B1. Together these results would suggest that DOC excreted in exponential growth was actually less labile in terms of its consumption rate vs. material likely derived from senescence, however at the same time of higher “quality” as a nutrient source for bacterial biomass formation. While somewhat speculative based on such a small comparison, this result does seem consistent with previous literature suggesting that the quality of the DOC, rather than the rate of supply, may regulate BGE in natural aquatic systems (Vallino et al., 1996).

3.3. Changes in THAA and D/L amino acid ratios in HMWDOC

As noted above (Materials and methods section) sample requirements for molecular-level AA isotopes required the isolation of the HMWDOC fraction by ultra-filtration. HMWDOC dominates the “semi-labile” DOM pool in aquatic systems, and so appears to be a more important source of C and energy for bacterial growth and respiration than LMWDOC (e.g. Amon and Benner, 1994, 1996; Gardner

et al., 1996). While the overall chemical composition of HMWDOC is typically similar to the total DOM pool, it also has younger ^{14}C ages (consistent with assumed greater reactivity), and differs in a number of additional molecular level properties (e.g., Benner et al., 1992; McCarthy et al., 1996; Walker et al., 2011). Our main goal here is to specifically investigate molecular-level isotopic effects of bacterial degradation on the dissolved hydrolysable AA from DOM. Therefore we first examined changes in several key AA indexes for bacterial degradation in the ultra-filtered DOM fraction, providing a basis for comparing $\delta^{15}\text{N}$ -AA changes with more established proxies.

Table 1 shows the evolution of THAA concentrations, individual AA mol% composition and D/L ratios of those AA with major D contributions, in both barrels, along bacterial incubations. THAA concentrations and D/L ratios of AA in HMW-DOM showed dramatic and statistically significant ($P < 0.1$) changes throughout the course of the degradation experiment (Table 1, Fig. 4). THAA concentrations were initially higher in B2 vs. B1, consistent with the elevated percentage of HMWDOC, and decreased rapidly after inoculation, reaching very low values ($4\text{--}44 \text{ nmol L}^{-1}$) after 15–16 days (Fig. 4, circles w/ lines). C normalized yields of THAA from HMWDOC fraction also decreased substantially in both barrels during degradation, reaching values of 0.05–0.74% after 15–16 days. At the same time, there was a parallel strong increase in the contribution of D-AA to the THAA pool (Fig. 4, filled bars), consistent with expectations from the literature for bacterial decomposition and reworking of DOC (e.g., Jiao et al., 2010; Kaiser and Benner, 2008; McCarthy et al., 1998; Nagata, 2000; Shleifer and Kandler, 1972).

The dramatic change in proportion of D vs. L amino acids during DOC decomposition (Table 1 and Fig. 4) may be related to two independent, but complimentary factors. The first factor is the relative increase in direct microbial sources. D-AA, in particular increases in D-Ala, D-Glx and D-Asx, are characteristics of marine DOM (e.g., Lee and Bada 1977, McCarthy et al., 1998; Kaiser and Benner, 2008), and have commonly been interpreted to indicate the accumulation of peptidoglycan remnants, or more generally bacterial-derived cell wall material (e.g., Grutters et al., 2002; McCarthy et al., 1998; Nagata, 2000; Pérez et al., 2003). However, the full range of specific D-AA we measured also includes some D-AA not previously reported as significant in the marine literature. Several were previously detected as minor D-forms in some oceanic regions [i.e. D-Ile in the Sargasso Sea (Lee and Bada, 1977); D-Leu in the Equatorial Pacific (Lee and Bada, 1977; McCarthy et al., 1998); D-Phe in the Gulf of Mexico (McCarthy et al., 1998)]. A much more diverse range of D-AA have also been recently reported in microbial natural products different than cell wall peptidoglycan sources (Cava et al., 2011; Vranova et al., 2012).

A second related factor could also be different cycling rates of D vs. L AA (e.g., Amon et al., 2001), with relatively slower remineralization and recycling of D-AA containing biomolecules leading to progressive increases in D/L ratios with continued degradation. The fact that the largest increases in D/L ratios occurred in both barrels between the second and third week of incubation (T2 to T3, Fig. 4), well after the bacterial abundance had crashed (Fig. 3), suggests that relative recycling rates may in fact be responsible for the very high D/L values observed at T3. Together, the D/L data suggests that the degree of microbial alteration at the last time point in these experiments may surpass that typically found in ocean regions where past work has been conducted, such that minor D-AA were increasingly expressed. Overall, while the strong increase in D-AA (including those typically seen in marine DOM) clearly indicates bacterial degradation, the range in D-AA species we observe suggests that bacterially-derived D-AA in the ocean may be more diverse than is currently recognized, as has been recently suggested (Kaiser and Benner, 2008).

Changes in AA mol% and in DI index values were also in agreement with those expected for progressive bacterial degradation. The DI index values (discussed in more detail in Section 3.8) were consistent with degraded material in all samples (Table 3), and decreased further with incubation in both barrels, consistent with increasing degradation state of remaining HMWDOM. DI value of -1.7 for our HMWDOM material at B1 after bacterial decomposition (Table 3) was very similar to

values reported by Yamashita and Tanoue (2003) for coastal surface waters (~ -1.7). Relative increases in the abundance (mol%) of Gly and Ala have also been shown in previous studies to be associated with diagenetically altered DOM (Amon et al., 2001; Dauwe et al., 1999; Dittmar et al., 2001; Yamashita and Tanoue, 2003). Accordingly, a gradual increase in Gly mol% was also observed with bacterial decomposition in both barrels (Table 1) and it was one of the three most abundant AA after degradation, consistent with oceanic observations (Hubberten et al., 1995; McCarthy et al., 1996; Yamashita and Tanoue, 2003). Ala mol% also increased after first week of incubation (period of maximum bacterial growth), in both barrels, however it then dropped strongly after 15–16 days (Table 1), coincident with near complete THAA degradation and very low bacterial numbers. While it is beyond the scope of our experimental design to interpret such finer details, overall the progressive trends for D-AA, DI index, and the Mol% of specific bacterial marker AA of isolated HMWDOM are all consistent with those for degraded organic material in the natural environment and indicate increasing contributions of bacterial biomass.

3.4. Amino acid compound specific isotopic ratios

To our knowledge this is the first study to directly examine compound-specific AA changes induced by heterotrophic bacterial degradation in any oceanic environment, and only the second (after Fogel and Tuross, 1999) in any context. Due to rapidly decreasing THAA concentrations, $\delta^{15}\text{N}$ -AA analyses were only possible at the first two time points of incubation; i.e., day 1 (T1) and day 8 or 9 (T2, for B1 and B2, respectively). We noted that the D/L ratios at T2 (Table 1), ranging from 0.01 to 0.63, are generally more similar to those found in oceanic HMWDOM, ranging from 0.04 to 0.61, (McCarthy et al., 1998), so this time point may also be a closer comparison to the extent of natural degradation. As noted above (Materials and methods) we have followed current literature convention in ordering our AA $\delta^{15}\text{N}$ results into Trophic vs. Source AA groups (Fig. 5), a division based on observed behavior of $\delta^{15}\text{N}$ values with trophic transfer in animals (e.g., McClelland and Montoya, 2002; Popp et al., 2007). While we do not expect animal trophic transfer to be directly relevant to bacterial degradation, it has recently been observed that the basic source vs. trophic-AA division also closely corresponds to the relative $\delta^{15}\text{N}$ fractionation of AA in autotrophic algae (Lehman, 2009), suggesting that this division may in fact represent a fundamental baseline in both autotrophic and heterotrophic sources. Further, an important question for many emerging $\delta^{15}\text{N}$ -AA applications (e.g., Sherwood et al., 2011) is to what degree bacterial degradation may alter information about ecosystem trophic structures based on trophic vs. source-AA value offsets. Therefore, this presentation simultaneously makes our data directly comparable to recent work, and highlights implications for many evolving CSI-AA applications.

3.5. $\delta^{15}\text{N}$ -AA patterns in excreted HMWDOM

The initial $\delta^{15}\text{N}$ -AA patterns from the freshest HMWDOM produced during exponential growth (B1, T1 in Fig. 5) are very similar to expectations from prior results from diverse plankton (e.g., Macko et al., 1987; McCarthy et al., 2007; McClelland and Montoya, 2002; Lehman, 2009). We did not directly measure the $\delta^{15}\text{N}$ -AA patterns of algal cell biomass from our experiments, primarily because our main goal was to examine changes in the DOM pool; however, the close correspondence of $\delta^{15}\text{N}$ -AA patterns in the freshest HMWDOM to literature values at least suggests little offset between biomass and excreted dissolved material. In fresh algal biomass trophic-AA group $\delta^{15}\text{N}$ values typically fall within a relatively similar band relative to the Glx $\delta^{15}\text{N}$ value. This is because Glx represents the central N pool for the cell, and the main source of N for transamination to all other AA (e.g., Hayes, 2001). In contrast, source-AA group $\delta^{15}\text{N}$ values are almost always depleted vs. Glx because they increasingly express isotopic fractionation characteristic of the enzymatic transamination reaction (Macko et al., 1986, 1987;

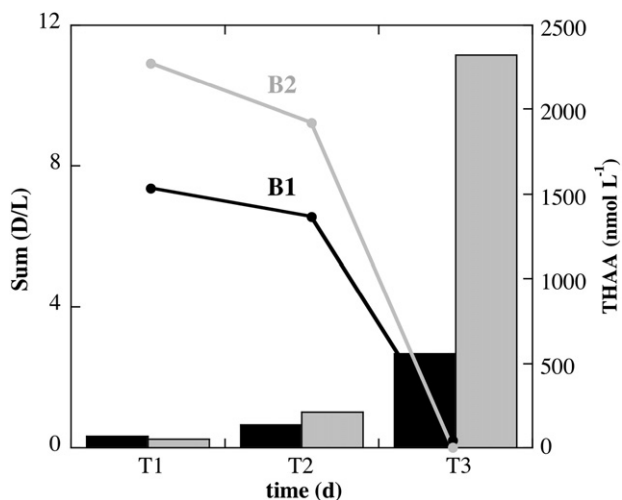


Fig. 4. The relationship of the sum of D/L ratios from all amino acids ($\Sigma(D/L)_{\text{all AA}}$, bars), and the concentration of total hydrolyzable amino acids (THAA, circles; nmol L^{-1}), with bacterial incubation time (T1, beginning of the incubation; T2, after 8–9 days; T3, after 15–16 days) in barrel 1 (B1, black bars and circles) and barrel 2 (B2, gray bars and circles).

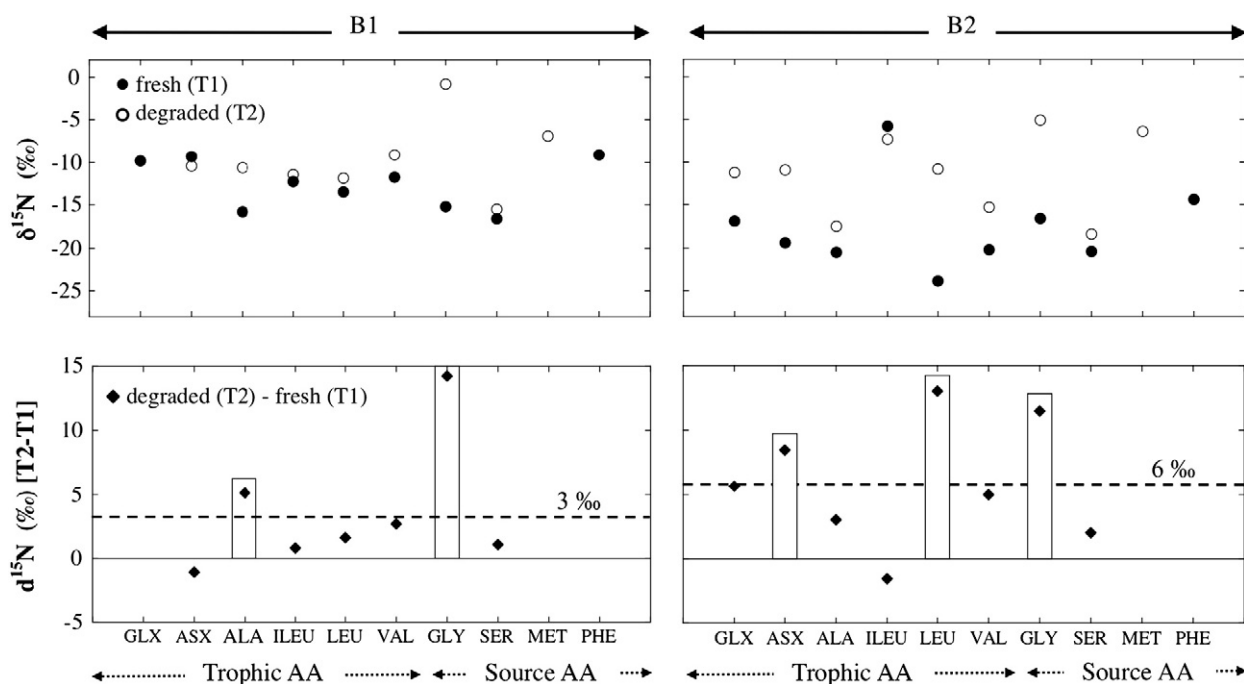


Fig. 5. $\delta^{15}\text{N}$ amino acid values ($\delta^{15}\text{N}$ -AA) for high molecular weight dissolved organic matter before and after bacterial degradation. Top panels: (A, B) show measured $\delta^{15}\text{N}$ -AA values of fresh HMWDOM, at start of degradation (T1, full circles) vs. degraded HMWDOM after 8–9 days (T2, empty circles) in barrel 1 (B1) and barrel 2 (B2) respectively. Lower panels: (C, D) show the corresponding differences $\delta^{15}\text{N}$ in value for each AA due to degradation (diamonds). Light line represents the zero line; i.e., the value if no $\delta^{15}\text{N}$ value change had occurred with degradation. Heavy dashed lines indicate the average value of $\delta^{15}\text{N}$ differences for all AA (3‰ for B1 and 6‰ for B2). Amino acids with much higher $\delta^{15}\text{N}$ offsets than average are highlighted with open bars. (n.b.: as described in text, due to very rapid AA degradation it was not possible to make $\delta^{15}\text{N}$ -AA at the last time point (T3) shown in previous figures).

Lehman, 2009). The $\delta^{15}\text{N}$ -AA pattern in our “freshest” end-member (B1, T1; Fig. 5) corresponds well with these expectations. Ala appears to be a sole exception within the trophic-AA group. Its depletion vs. Glx could be due to bacterial degradation that had already occurred at harvest, however depleted Ala $\delta^{15}\text{N}$ values have also previously been observed in at least a few eukaryotic algal species (Lehman, 2009). Within the source-AA group, Phe has $\delta^{15}\text{N}$ values similar to Glx, therefore somewhat higher than typical for most prior $\delta^{15}\text{N}$ -AA patterns in plankton biomass. It is also possible that these values are related to early bacterial alteration, a hypothesis possibly supported by initial negative DI values. However at the same time, Phe is amongst the least abundant AA here (2–4 mol%, Table 1), and these values could therefore be subject to additional error.

Overall, while we cannot discount some influence of bacterial degradation in our “freshest” HMWDOM, the overall similarity of $\delta^{15}\text{N}$ -AA pattern vs. those previously reported for algal biomass (e.g., McCarthy et al., 2007) suggests that HMWDOM excreted during exponential algal growth has similar $\delta^{15}\text{N}$ -AA patterns as those expected from bulk algal cells. Certainly when compared to the strongly changed $\delta^{15}\text{N}$ -AA patterns evident with degradation (Fig. 5, T2), the $\delta^{15}\text{N}$ -AA pattern in HMWDOM from B1 at T1 indicates the experiment has largely captured a “fresh” plankton end-member. This observation suggests that excreted algal DOM would likely have very similar $\delta^{15}\text{N}$ -AA patterns as bulk cells, with implications for the interpretation of $\delta^{15}\text{N}$ -AA patterns in natural DOM pool (McCarthy et al., 2007). This seems reasonable bio-chemically, since all cellular AA are the products of the same central metabolic pathways, however it has never been previously demonstrated.

3.6. Change in $\delta^{15}\text{N}$ -AA with microbial degradation

Major differences were observed between the fresher (T1) and more degraded (T2) HMWDOM samples in both barrels (Fig. 5), and all the

degraded $\delta^{15}\text{N}$ -AA patterns were also strongly shifted vs. the relatively uniform $\delta^{15}\text{N}$ -AA patterns characteristic of fresh plankton biomass (Lehman, 2009) discussed above. An average enrichment of 3‰ and 6‰ after degradation for total proteinaceous material was observed in B1 and B2 respectively (Figs. 5 and 6). In contrast with the unidirectional enrichment of only the Tr-AA group that characterizes trophic transfer in animals (e.g., Chikaraishi et al., 2009; McClelland and Montoya, 2002), there was no obvious relationship between AA with strongly altered $\delta^{15}\text{N}$ values, and the trophic vs. source-AA groupings. Further, the $\delta^{15}\text{N}$ -AA patterns at T2 in each barrel are quite different. In B1, the strongest individual AA fractionations were observed in Ala and Gly, while most other $\delta^{15}\text{N}$ values were more modestly elevated. In contrast at B2, at both T1 and T2 $\delta^{15}\text{N}$ -AA patterns were very different from the “fresh” material, and also from patterns expected in algae. In the most degraded HMWDOM sample (B2 T2, according to D/L ratios and DI values, Table 3), Asx, Leu and Gly stood out as having extremely strong fractionations (7–15‰ in T2 vs. T1), however most AA $\delta^{15}\text{N}$ values were also substantially elevated.

Overall, these changes strongly support the hypothesis that bacterial degradation results in a “scattering” of the autotrophic $\delta^{15}\text{N}$ -AA patterns (McCarthy et al., 2007). In contrast to trophic transfer in animals, the metabolic diversity of microorganisms allows either salvage incorporation or resynthesis of any AA. Therefore, McCarthy et al. (2007) hypothesized that the exact effects of bacterial degradation on $\delta^{15}\text{N}$ -AA patterns may be highly variable, depending on exact growth conditions and the range of substrates available. However, because a relatively consistent $\delta^{15}\text{N}$ -AA pattern characterizes autotrophs, any bacterial AA resynthesis should also fundamentally alter (“scatter”) the $\delta^{15}\text{N}$ -AA pattern. This increase in “scatter” vs. autotrophic source patterns is quantified as the ΣV parameter (McCarthy et al., 2007; discussed in more detail below). The clear changes to the $\delta^{15}\text{N}$ -AA pattern in our degradations, with higher ΣV values in degraded HMWDOM samples (3.7‰) vs. “fresh” samples (2.4‰)

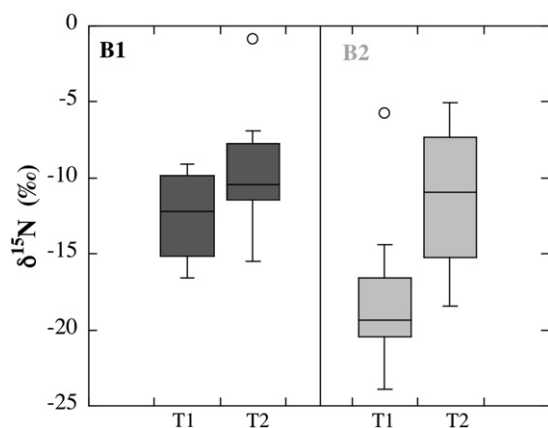


Fig. 6. Distribution of mol% weighted average $\delta^{15}\text{N}$ amino acid values (‰) before (T1) and after (T2) bacterial degradation in barrel 1 (B1) and barrel 2 (B2). Changes in both barrels show the clear increase in $\delta^{15}\text{N}$ value of average proteinaceous material with bacterial degradation. The horizontal line in the boxes represents the median, the boxes extend from the 25% to the 75% quartile of the data distribution, and the vertical lines indicate the 5% and 95% quartiles. Open circles represent individual data that falls below or above the 5% and 95% quartiles.

(Table 3), as well as differences in exact results between B1 and B2, are both consistent with these ideas. Further, these results are also consistent with previous data for oceanic organic matter (McCarthy et al., 2007), where the large differences observed in overall “scatter” of $\delta^{15}\text{N}$ -AA values between plankton (ΣV ranging from 1 to 1.5 ‰) and more degraded sediment trap samples (ΣV ranging from 1.4 to 3.4‰) were suggested to be linked to continuing bacterial resynthesis. Similarly, Fogel and Tuross (1999) first observed that $\delta^{15}\text{N}$ -AA patterns in fresh plant protein had a narrow range of values, whereas degraded material was also highly “scattered” (in that experiment, fractionation was observed in almost every amino acid by differences of up to 15‰). Overall our observations confirm that HMWDOM pool in both degradations contain AA which have been resynthesized by bacteria, likely incorporating new nitrogen directly into the proteinaceous AA pool with large isotopic fractionation.

The $\delta^{15}\text{N}$ values changes for several AA also stand out within these overall results. It is notable (and unfortunate) that due to very low concentrations at T2 in both barrels (due to rapid AA utilization) we were not able to measure Phe $\delta^{15}\text{N}$ values in either sample of degraded HMWDOM. The Phe $\delta^{15}\text{N}$ is the AA which has been proposed as the best tracer for $\delta^{15}\text{N}$ values at the base of foodwebs (e.g., Chikaraishi et al., 2009), therefore its alteration with microbial degradation has major implications for many paleoceanographic applications. Fogel and Tuross (1999) observed Phe to be the only AA whose $\delta^{15}\text{N}$ value did not change in their degradation experiments, however whether this is a general result remains an important open question. Finally, Gly $\delta^{15}\text{N}$ value was the only AA showing very large, and also consistent, fractionation in both experiments (14.3 ‰ in B1 and 11.5 ‰ in B2; Table 2, Fig. 5). While clearly only based on two cultures, this observation is also consistent with multiple previous studies which associate the abundance of Gly to diagenetically altered DOM (Amon et al., 2001; Dauwe et al., 1999; Dittmar et al., 2001; Yamashita and Tanoue, 2003), as well as our own Gly mol% data (Table 1). Very strongly fractionated Gly $\delta^{13}\text{C}$ values have also been observed in concert with elevated mol% in degraded ocean particles (McCarthy et al., 2004). These results suggest that together concentration, ^{13}C and ^{15}N isotopic fractionation of Gly may constitute robust tracers for heterotrophic bacterial reworking.

3.7. Overall $\delta^{15}\text{N}$ change in HMW proteinaceous material: implication for LMW and HMW DON in the oceans

A central result from both experiments is that the $\delta^{15}\text{N}$ values of individual AA in bacterially degraded material were generally shifted

to more positive $\delta^{15}\text{N}$ values (Fig. 6). In particular, every AA with a large fractionation between T1 and T2 was strongly enriched (5–15‰) in the more degraded HMWDOM. The only exceptions were Asx in B1 and Ile in B2, both shifted to slightly more negative $\delta^{15}\text{N}$ values (Fig. 4, lower panel). The relative shifts in $\delta^{15}\text{N}$ values of DON in microorganisms can be complex, depending in part on concentration and forms of inorganic N available (Hoch et al., 1996). Fogel and Tuross (1999) conducted degradation under conditions with very high ammonia concentrations (millimolar), and showed that bacteria can incorporate this nitrogen directly into AA, resulting in much lighter $\delta^{15}\text{N}$ signatures (Fogel and Tuross, 1999). However the ammonia concentrations in our experiments (0.9–1.9 $\mu\text{mol L}^{-1}$) were very low vs. those in these previous experiments (Hoch et al., 1992, 1996; Fogel and Tuross, 1999). Perhaps more important, these levels are similar to ranges expected for subsurface ocean (<5 $\mu\text{mol L}^{-1}$, Brzezinski, 1988). Our results are also consistent with the suggestion that bacterial decomposition of ocean DON generally causes $\delta^{15}\text{N}$ enrichment in residual material (Knapp et al., 2005, 2011). The average enrichments of 3‰ and 6‰ for total proteinaceous material observed in B1 and B2 respectively (Figs. 5 and 6) are therefore consistent with greater overall $\delta^{15}\text{N}$ enrichment corresponding with more advanced water column DON degradation.

The magnitude and direction of the average $\delta^{15}\text{N}$ isotope shifts we observed also correspond well with a recently proposed conceptual model which incorporates the microbial loop to explain observed $\delta^{15}\text{N}$ shifts in DON, and also the correspondence of $\delta^{15}\text{N}$ values between upper-ocean DON and subsurface nitrate (Knapp et al., 2011). In this hypothesis, DON is produced in the surface ocean by the solubilization of suspended PON without isotope fractionation. Subsequent microbial breakdown of DON then preferentially consumes the light (^{15}N depleted) substrate, resulting in substantial fractionation (roughly 3 to 5‰) in residual DON. Together, this produces a DON pool with elevated $\delta^{15}\text{N}$, and supplies regenerated dissolved inorganic nitrogen (DIN) with low $\delta^{15}\text{N}$ values back to the euphotic zone. The average bulk DON $\delta^{15}\text{N}$ values for 0 to 100 m reported in the North Atlantic and North Pacific basins (3.9‰ and 4.7‰ respectively, Knapp et al., 2005, 2011) are both slightly lower than the HMWDOM $\delta^{15}\text{N}$ also reported for similar sites (4.7‰ in the North Atlantic and 5.4‰ in the North Pacific, Meador et al., 2007). Both the model proposed by Knapp et al. (2011) and our results here would be consistent with enrichment in $\delta^{15}\text{N}$ of HMWDOM vs. LMWDOM. The recent work of Knapp and co-workers (Knapp et al., 2012), directly measuring for the first time the distinct nitrogen isotopic composition of both size fraction pools of DON, is also consistent with this hypothesis.

Our experimental data can also further constrain the mechanism for observed $\delta^{15}\text{N}$ changes. One possibility to explain ^{15}N -enriched HMWDOM is that, as in the hypothesis above, isotopic fractionation occurs due to direct cleavage of N-bonds with an associated fractionation (Knapp et al., 2011, 2012) produced by either photosynthetic and/or heterotrophic activity. Our results here strongly suggest that the reason for AA $\delta^{15}\text{N}$ increase is due to *resynthesis* by heterotrophic bacteria. The progressive incorporation of *bacterial-sourced* proteinaceous material into HMWDOM is consistent with the strong change in $\delta^{15}\text{N}$ -AA patterns (indicating resynthesis), coupled with simultaneously increasing D/L ratios and DI index values (Fogel and Tuross, 1999; McCarthy et al., 2007). It might be argued that selective hydrolysis of ^{15}N -depleted AA could also produce the changes in $\delta^{15}\text{N}$ -AA pattern we observe, however this would certainly not alter AA enantiomeric ratios. Since enantiomeric ratios in natural ocean HMWDOM are also high, and presumed to unambiguously indicate bacterial biomass input (Kaiser and Benner, 2008; McCarthy et al., 1997), we propose that heterotrophic bacterial origin is an alternate explanation for elevated $\delta^{15}\text{N}$ values of HMWDOM, which ties together changes in $\delta^{15}\text{N}$ values with broader biomarker data. While this may seem like a subtle mechanistic difference, it has important implications for understanding the role of ocean bacteria in creating refractory dissolved

Table 2

Compound-specific $\delta^{15}\text{N}$ values for individual amino acids in barrel 1 (B1) and barrel 2 (B2) at the two incubation time points (T1 and T2, 1 and 8–9 days respectively) for which amino acids remained abundant enough for isotopic measurements. AA abbreviations are as defined in the [Materials and methods](#).

Experiment	Time (d)	Trophic AA						Source AA			
		Glx	Asx	Ala	Ileu	Leu	Val	Gly	Ser	Met	Phe
B1T1	1	-9.8 ± 1.4	-9.3 ± 1.1	-15.8 ± 0.9	-12.2 ± 1.4	-13.4 ± 1.2	-11.8 ± 1.0	-15.1 ± 2.5	-16.6 ± 1.9	n.d.	-9.1 ± 0.8
B1T2	8	n.d.	-10.4 ± 1.0	-10.6 ± 0.4	-11.4 ± 1.6	-11.9 ± 0.7	-9.1 ± 1.0	-0.8 ± 1.2	-15.5 ± 1.1	-6.9 ± 1.1	n.d.
B2T1	1	-16.8 ± 2.0	-19.4 ± 0.2	-20.5 ± 2.5	-5.7 ± 1.7	-23.9 ± 0.6	-20.2 ± 0.6	-16.6 ± 1.6	-20.4 ± 0.5	n.d.	-14.4 ± 1.9
B2T2	9	-11.2 ± 1.7	-10.9 ± 0.7	-17.4 ± 0.9	-7.3 ± 0.9	-10.8 ± 0.7	-15.2 ± 0.5	-5.1 ± 1.4	-18.4 ± 1.2	-6.4 ± 1.4	n.d.

material (Jiao et al., 2010), as well as possibly shaping the isotopic signature of the oceans DON pool.

At the same time, the literature suggests that at some ocean locations the differences documented between $\delta^{15}\text{N}$ values of PON, DON and HMWDON are small; in particular for HMWDON, little difference has been observed with increasing depth at some oceanic sites (Benner et al., 1997; Meador et al., 2007). These authors hypothesized that this lack of molecular-isotopic change with depth, at least for HMW fraction, indicates that its AA composition was largely “preformed” due to surface ocean biological processes, and/ or that autotrophic prokaryotes might be major additional sources. In light of our observations here, these results seem somewhat puzzling. However, we note that earlier DON $\delta^{15}\text{N}$ -AA measurements were also not able to measure as many AA, nor with as great precision, as we have in the current study. Future experiments coupling ancillary proxies simultaneously with $\delta^{15}\text{N}$ -AA measurements from different DON size fractions may be able to clarify these issues.

3.8. D/L ratio, DI and ΣV parameters: complimentary proxies for degradation and bacterial resynthesis

$\delta^{15}\text{N}$ -AA patterns can provide a direct understanding of proteinaceous $\delta^{15}\text{N}$ value change at the molecular level due to degradation. As noted above, the ΣV parameter has been proposed by McCarthy et al. (2007) to track the degree of bacterial AA resynthesis. This represents fundamentally different mechanistic information vs. that carried by the more traditional proxies such as the DI index (providing information on OM degradation state, based in mol% composition of AA), or D/L ratios (allowing the identification of OM most probable bacterial vs. algal sources). Simultaneously examining ΣV , DI, and D/L ratios may therefore provide a new level of detail into the role of heterotrophic bacteria in shifting bulk isotopic values, as well as creating refractory organic matter.

Decreasing values of DI indicate increasing degradation state, and it has been widely used to determine OM general reactivity in particles (e.g., Amon et al., 2001; Davis and Benner, 2007; McCarthy et al., 2007; Yamashita and Tanoue, 2003). However, mechanistically, DI changes are ambiguous: changing mol% distribution could equally be due to selective remineralization, or to in-growth of bacterially-derived material with unique composition. DI values derived from THAA measured in our experiment were negative in all HMWDOM samples analyzed (Table 3). Since exact DI values can vary depending on the specific AA quantified by different methods, comparing only DI trends is likely most robust. Starting HMWDOM from B2 (before bacterial incubation) yielded substantially more negative DI values (-1.6) vs. that from B1 (-1.4), presumably because the senescent growth conditions yielded more degraded initial material, as indicated by the lower C normalized yield of THAA at B2, in comparison with that at B1. In both barrels the DI index of HMWDOM after bacterial incubation shifted to more negative values (Table 3) and, accordingly, C normalized yield of THAA decreased drastically within the first two weeks of incubation. Together, these trends and DI values are all consistent with assumptions of degradation discussed above for the two barrels. This result indicates

that mol% composition of the HMWDOM pool has changed substantially on a time scale of days, due either to selective remineralization, or to the resynthesis/incorporation of new bacterially-derived proteinaceous material with characteristically different mol% composition.

The ΣV parameter has no direct connection to AA mol%. Instead, if proteinaceous sources have the same $\delta^{15}\text{N}$ -AA patterns (as in this study), then ΣV indicates progressive change away from the $\delta^{15}\text{N}$ -AA distribution characteristic of primary producers. If mixtures can be ruled out (as in this experiment), such shifts in AA $\delta^{15}\text{N}$ values indicate microbial resynthesis (McCarthy et al., 2007). Therefore, an observed change in ΣV likely indicates the incorporation of new bacterial biosynthate into the HMWDOM pool. Note, however, that ΣV is only affected if resynthesis changes isotopic value.

Together, the interpretation made possible by DI, ΣV , and D/L ratios together allows the most detailed view into HMWDOM degradation processes in our experiments. In B1, all three change in concert, and are consistent with bacterial degradation simultaneously increasing the overall $\delta^{15}\text{N}$ value of proteinaceous material (Table 3, Fig. 6) via the incorporation of new bacterially-produced material. In contrast, in B2 the parameters diverge. Starting HMWDOM in B2 was apparently already substantially bacterially degraded, and the rapid additional degradation which occurred caused a further (and larger) increase in overall $\delta^{15}\text{N}$ value (Fig. 6, Table 3). This was also coupled with a larger change in DI index, and a larger increase in D/L ratios (Fig. 4, Table 3) vs. B1. However, the ΣV values remained essentially unchanged (Table 3). This contrast suggests one limitation of the ΣV parameter: because it summarizes changes in $\delta^{15}\text{N}$ -AA pattern, if $\delta^{15}\text{N}$ -AA values change in a relatively unidirectional way, then ΣV will not be strongly changed. In B2, the ΣV value appears to capture the relatively advanced bacterial degradation state in the senescent culture at time of harvest, but not its further degradation.

It is also interesting to note that this difference in ΣV between the two barrels also corresponds with similar differences in the BGE evolution data. In B1 the BGE is calculated to be ~60%, indicating that most of the carbon consumed is being incorporated into new bacterial biomass, necessarily implying that AA are also being incorporated.

Table 3

Summary of amino acid and bacterial growth parameters for barrel 1 (B1) and barrel 2 (B2). Degradation Index (DI), summed D/L ratio (ΣD), ΣV resynthesis parameter (%), and the mol%-weighted average $\delta^{15}\text{N}$ value for all hydrolyzable AA ($\delta^{15}\text{N}_{\text{avg}}$ (‰)), are given for the initial time (T1) and after degradation (T2). The change in each parameter (Δ) between T1 and T2 ($\Delta = \text{T2} - \text{T1}$), along with calculated Bacterial Growth Efficiency (BGE, %) and CO_2 yields (%), for each barrel, are shown in the middle column.

	B1			B2		
	T1	Δ	T2	T1	Δ	T2
BGE (%)			60			18
CO_2 yield (%)			40			82
DI	-1.4	-0.3	-1.7	-1.6	-0.7	-2.4
$\Sigma\text{D/L}$	0.3	0.3	0.7	0.3	0.8	1.0
ΣV (%)	2.4	0.6	3.0	3.7	n.d.	3.7
$\delta^{15}\text{N}_{\text{avg}}$ (‰)	-12.5	2.9	-9.6	-18.9	6.3	-12.5

This seems consistent with ΣV increase in B1, since strong heterotrophic AA resynthesis might be expected to agree with high BGE. In B2, however, ΣV does not significantly increase, and, accordingly, BGE is much lower (~18%). Thus in B2, even as HMWDOC is being degraded (and as DI index increases), more organic matter is remineralized vs. incorporated into bacterial biomass.

Overall these results strongly support the idea that ΣV can indicate bacterial resynthesis, but also suggest it may not be “linear” with degradation. The relatively limited data available here is clearly an important caveat for detailed interpretation, and future degradation experiments in diverse conditions will be needed to provide a firmer basis for ΣV interpretation. Based on our results, it is also possible that specific AA (for example, the $\delta^{15}\text{N}$ value of Gly), or selected subset of bacterial indicator AA, may turn out to be more consistent indicators of heterotrophic bacterial resynthesis than the total $\delta^{15}\text{N}$ -AA pattern. However, in complex natural samples, any approach based on evaluating only a few specific $\delta^{15}\text{N}$ values may be unwise. Therefore the ΣV parameter, coupled with close examination of $\delta^{15}\text{N}$ -AA vs. the expected autotrophic patterns, may be among the best way to evaluate microbial resynthesis in complex natural systems.

4. Concluding remarks

A main frontier in marine biogeochemistry is the need to understand the effects of microbial heterotrophy on the dissolved organic pool in the oceans (e.g., Azam and Worden, 2004; Jiao et al., 2010; McCarthy et al., 1997; Ogawa et al., 2001). Transformations within microbial food webs are increasingly recognized as likely key in creating recalcitrant dissolved molecules, which ultimately regulate the storage of reduced C and N in the ocean's interior (Jiao et al., 2010). Specifically for DON, microbially-mediated change may be the central mechanism for the redistribution of ^{15}N in the water column, in particular in the euphotic zone where microbial activity could account for discrepancies observed in ^{15}N budgets (Knapp et al., 2011, 2012; Somes et al., 2010). While clearly the data we report here are first experiments, these findings break new ground in suggesting a direct mechanistic explanation for changes in $\delta^{15}\text{N}$ values observed in the DON pool, and possibly also for $\delta^{15}\text{N}$ offsets between DON molecular weight fractions.

The increase we observed in average $\delta^{15}\text{N}$ value of total AA pool with bacterial degradation is consistent with recent observations for both DON and HMWDON $\delta^{15}\text{N}$ (Knapp et al., 2005, 2011) and strongly points toward a central role for bacterial heterotrophy in explaining this change. Specifically, our data suggests that incorporation of bacterial proteinaceous material into the DON pool, vs. the isotopic fractionation of algal production, is more likely as a main mechanism for DON $\delta^{15}\text{N}$ value changes. This difference implies that the cycling of N (and presumably C) through bacterial biomass may be the key process controlling preservation of DON. If correct, this conclusion would add to accumulating recent work on the importance of the “microbial carbon pump” as a framework for regulation of flux and preservation of DOM in the deep sea (e.g., Jiao et al., 2011 and references therein).

Most broadly, our results indicate new potential for $\delta^{15}\text{N}$ -AA measurements to provide a detailed window into mechanisms of microbial degradation on organic matter pools. We propose that $\delta^{15}\text{N}$ -AA measurements can reveal the direct molecular-level basis for bulk $\delta^{15}\text{N}$ values, and also $\delta^{15}\text{N}$ change, in proteinaceous material, which in turn makes up the large majority of detrital ON in POM, recent sediments, and subsurface DON (e.g., Hedges et al., 2001; Knicker and Hatcher, 2001; McCarthy et al., 1996).

Finally, for the ocean DON pool specifically, this research suggests that $\delta^{15}\text{N}$ -AA coupled with ancillary AA analyses and with parameters for bacterial growth, may provide significant new insight into marine DON at different stages of microbial transformation. Measuring DON $\delta^{15}\text{N}$ -AA patterns in contrasted ocean regions and depths, coupled with specific AA biomarkers for processes occurring within the

microbial loop, may be a particularly powerful approach, due to the large fractionations observed in individual AA vs. far smaller shifts expected for bulk $\delta^{15}\text{N}$ values. At the same time, considering bacterial growth efficiency and trends in CO_2 yields during DOC consumption may help resolve uncertainties about respiration and dynamics of organic carbon and nitrogen in the deep ocean (Aristegui et al., 2002; del Giorgio and Duarte, 2002). Further experimental and field data is needed in order to reinforce this work, and to confirm compound specific constraints for tracking DON sources and bacterial reworking signatures in the open ocean.

Acknowledgments

This research is a contribution to the “Amino acid molecular-level stable isotopic and enantiomeric ratios: a new approach for understanding source and transformation of organic nitrogen in the sea” project, funded by the National Science Foundation, OCE 0623622. We thank J. Lehman, B. Walker, L. Roland and Y. Sano for help and advice with laboratory work. M.L.C. was supported by the Agency for Administration of University and Research Grants (AGAUR, grant 2007 BP-A 00156), and by the Spanish Research Council with a JAEDOC grant (JAEDOC030).

References

- Amon, R.M.W., Benner, R., 1994. Rapid cycling of high-molecular-weight dissolved organic matter in the ocean. *Nature* 369, 549–552.
- Amon, R.M.W., Benner, R., 1996. Bacterial utilization of different size classes of dissolved organic matter. *Limnol. Oceanogr.* 41, 41–51.
- Amon, R.M.W., Fitznar, H.P., Benner, R., 2001. Linkages among the bioreactivity, chemical composition, and diagenetic state of marine dissolved organic matter. *Limnol. Oceanogr.* 46, 287–297.
- Andrews, P., Williams, P.J.L., 1971. Heterotrophic utilization of dissolved organic compounds in the sea. *J. Mar. Biol. Assoc. U. K.* 51, 111–125.
- Aristegui, J., Duarte, C.M., Agustí, M., Doval, M., Álvarez-Salgado, X.A., Hansell, D.A., 2002. Dissolved organic carbon support of respiration in the dark ocean. *Science* 298 (5600), 1967. <http://dx.doi.org/10.1126/science.107674>.
- Azam, F., Malfatti, F., 2007. Microbial structuring of marine ecosystems. *Nat. Rev. Microbiol.* 5, 782–791.
- Azam, F., Worden, A.Z., 2004. Microbes, molecules, and marine ecosystems. *Science* 303, 1622–1624.
- Benner, R., 2002. Chemical composition and reactivity. In: Hansell, D., Carlson, C. (Eds.), *Biogeochemistry of Dissolved Organic Matter*. Academic Press, Amsterdam, pp. 59–90.
- Benner, R., Pakulski, J.D., McCarthy, M., Hedges, J.I., Hatcher, P.G., 1992. Bulk chemical characteristics of dissolved organic matter in the ocean. *Science* 255, 1561–1564.
- Benner, R., Strom, M., 1993. A critical evaluation of the analytical blank associated with DOC measurements by high temperature catalytic oxidation. *Mar. Chem.* 41, 153–160.
- Benner, R., Biddanda, B., Black, B.M., McCarthy, M., 1997. Abundance, size distribution, and stable carbon and nitrogen isotope compositions of marine organic matter isolated by tangential-flow ultrafiltration. *Mar. Chem.* 57, 243–263.
- Berman, T., Bronk, D.A., 2003. Dissolved organic nitrogen: a dynamic participant in aquatic ecosystems. *Aquat. Microb. Ecol.* 31 (3), 279–305. <http://dx.doi.org/10.3354/ame031279>.
- Bevington, P.R., Robinson, D.K., 2003. *Data Reduction and Error Analysis for the Physical Sciences*. McGraw-Hill.
- Biddanda, B., Benner, R., 1997. Carbon, nitrogen, and carbohydrate fluxes during the production of particulate and dissolved organic matter by marine phytoplankton. *Limnol. Oceanogr.* 42 (3), 506–518.
- Biersmith, A., Benner, R., 1998. Carbohydrates in phytoplankton and freshly produced dissolved organic matter. *Mar. Chem.* 63, 131–144.
- Brzezinski, M.A., 1988. Vertical distribution of ammonium in stratified oligotrophic waters. *Limnol. Oceanogr.* 33 (5), 1176–1182.
- Carlson, C.A., 2002. Production and consumption processes. In: Hansell, D., Carlson, C. (Eds.), *Biogeochemistry of Dissolved Organic Matter*. Academic Press, San Diego, pp. 91–151.
- Cava, F., Lam, H., de Pedro, M.A., Waldor, M.K., 2011. Emerging knowledge of regulatory roles of D-amino acids in bacteria. *Cell. Mol. Life Sci.* 68, 817–831. <http://dx.doi.org/10.1007/s00018-010-0571-8>.
- Chikaraishi, Y., Ogawa, N.O., Kashiyama, Y., Takano, Y., Suga, H., Tomitani, A., Miyashita, H., Kitazato, H., Ohkouchi, N., 2009. Determination of aquatic food-web structure based on compound-specific nitrogen isotopic composition of amino acids. *Limnol. Oceanogr. Methods* 7, 740–750.
- Cowie, G.L., Hedges, J.I., 1992. Sources and reactivities of amino acids in a coastal marine environment. *Limnol. Oceanogr.* 37 (4), 703–724.
- Cowie, G.L., Hedges, J.I., 1994. Biochemical indicators of diagenetic alteration in natural organic matter mixtures. *Nature* 369, 304–307.
- Dauwe, B., Middelburg, J.J., 1998. Amino acids and hexosamines as indicators of organic matter degradation state in North Sea sediments. *Limnol. Oceanogr.* 43 (5), 782–798.

- Dauwe, B., Middelburg, J.J., Herman, P.M.J., Heip, C.H.R., 1999. Linking diagenetic alteration of amino acids and bulk organic matter reactivity. *Limnol. Oceanogr.* 44 (7), 1809–1814.
- Davis, J., Benner, R., 2007. Quantitative estimates of labile and semi-labile dissolved organic carbon in the western Arctic Ocean: a molecular approach. *Limnol. Oceanogr.* 52 (6), 2434–2444.
- Davis, J., Kaiser, K., Benner, R., 2009. Amino acid and amino sugar yields and compositions as indicators of dissolved organic matter diagenesis. *Org. Geochem.* 40, 343–352.
- del Giorgio, P.A., Cole, J.J., 1998. Bacterial growth efficiency in natural aquatic systems. *Annu. Rev. Ecol. Syst.* 29, 503–541.
- del Giorgio, P.A., Duarte, C.M., 2002. Respiration in the open ocean. *Nature* 420, 379–384.
- Dittmar, T., Fitznar, H.P., Kattner, G., 2001. Origin and biogeochemical cycling of organic nitrogen in the eastern Arctic Ocean as evident from D- and L-amino acids. *Geochim. Cosmochim. Acta* 65 (22), 4102–4114.
- Fogel, M.L., Tuross, N., 1999. Transformation of plant biochemicals to geological macromolecules during early diagenesis. *Oecologia* 120, 336–346.
- Frank, H., Woiwode, W., Nicholson, G.J., Bayer, E., 1979. Determination of optical purity of amino acids in proteins. In: Klein, E.R., Klein, P.D. (Eds.), *Stable Isotopes, Proceedings of the Third International Conference*. Academic Press.
- Gardner, W.S., Benner, R., Amon, R.M.W., Cotner Jr., J.B., Cavaletto, J.F., Johnson, J.R., 1996. Effects of high-molecular-weight dissolved organic matter on nitrogen dynamics in the Mississippi River plume. *Mar. Ecol. Prog. Ser.* 133, 287–297.
- Grueters, M., van Raaphorst, W., Epping, E., Helder, W., de Leeuw, J.W., 2002. Preservation of amino acids from in situ-produced bacterial cell wall peptidoglycans in northeastern Atlantic continental margin sediments. *Limnol. Oceanogr.* 47 (5), 1521–1524.
- Guillard, R.R.L., Ryther, J.H., 1962. Studies on marine planktonic diatoms. I. *Cyclotella nana*. Hustedt and *Detonula confervacea* (Cleve) Gran. *Can. J. Microbiol.* 8, 229–239.
- Hayes, J.M., 2001. Fractionation of carbon and hydrogen isotopes in biosynthetic processes. In: Cole, D.R., Valley, J.W. (Eds.), *Stable Isotope Geochemistry*, 43. Mineralogical Society of America, pp. 225–278.
- Hedges, J.L., Baldock, J.A., Gelin, Y., Lee, C., Peterson, M.L., Wakeham, S.G., 2001. Evidence for non-selective preservation of organic matter in sinking marine particles. *Nature* 409, 801–804.
- Hedges, J.L., Baldock, J.A., Gelin, Y., Lee, C., Peterson, M.L., Wakeham, S.G., 2002. The biochemical and elemental compositions of marine plankton: a NMR perspective. *Mar. Chem.* 78, 47–63.
- Hoch, M.P., Fogel, M.L., Kirchman, D.L., 1992. Isotope fractionation associated with ammonium uptake by a marine bacterium. *Limnol. Oceanogr.* 37 (7), 1447–1459.
- Hoch, M.P., Snyder, R.A., Cifuentes, L.A., Coffin, R., 1996. Stable isotope dynamics of nitrogen recycled during interactions among marine bacteria and protists. *Mar. Ecol. Prog. Ser.* 132, 229–239.
- Hopkinson, C.S., Vallino, J.J., 2005. Efficient export of carbon to the deep ocean through dissolved organic matter. *Nature* 433, 142–145.
- Hubberten, U., Lara, R.J., Kattner, G., 1995. Refractory organic compounds in polar waters: relationship between humic substances and amino acids in the Arctic and Antarctic. *J. Mar. Res.* 53, 137–149.
- Jackson, G.A., Williams, P.M., 1985. Importance of dissolved organic nitrogen and phosphorus to biological nutrient cycling. *Deep-Sea Res.* 32 (2), 223–235.
- Jennerjahn, T.C., Ittekkot, V., 1997. Organic matter in sediments in the mangrove areas and adjacent continental margins of Brazil: I. Amino acids and hexosamines. *Oceanol. Acta* 20, 359–369.
- Jiao, N., Herndl, G.J., Hansell, D.A., Benner, R., Kattner, G., Wilhelm, S.W., Kirchman, D.L., Weinbauer, M.G., Luo, T., Chen, F., Azam, F., 2010. Microbial production of recalcitrant dissolved organic matter: long-term carbon storage in the global ocean. *Nat. Rev. Microbiol.* 8, 593–599.
- Jiao, N., Azam, F., 2011. Microbial Carbon Pump and its Significance for Carbon Sequestration in the Ocean. In: Jiao, N., Azam, F., Sanders, S. (Eds.), *Microbial Carbon Pump in the Ocean*. Science/AAAS Business Office, Washington, DC, p. 43–45.
- Jørgensen, N.O.G., Kroer, N., Coffin, R.B., Hoch, M.P., 1999. Relations between bacterial nitrogen metabolism and growth efficiency in an estuarine and an open-water ecosystem. *Aquat. Microb. Ecol.* 18, 247–261.
- Kaiser, K., Benner, R., 2005. Hydrolysis-induced racemization of amino acids. *Limnol. Oceanogr. Methods* 3, 318–325.
- Kaiser, K., Benner, R., 2008. Major bacterial contribution to the ocean reservoir of detrital organic carbon and nitrogen. *Limnol. Oceanogr.* 53, 99–112. <http://dx.doi.org/10.4319/lo.2008.53.1.0099>.
- Keil, R.G., Fogel, M.L., 2001. Reworking of amino acids in marine sediments: stable carbon isotopic composition of amino acids in sediments along the Washington coast. *Limnol. Oceanogr.* 46, 14–23.
- Knapp, A.N., Sigman, D.M., Lipschultz, F., 2005. N isotopic composition of dissolved organic nitrogen and nitrate at the Bermuda Atlantic Time-series Study site. *Global Biogeochem. Cycles* 19, GB1018. <http://dx.doi.org/10.1029/2004GB002320>.
- Knapp, A.N., Sigman, D.M., Lipschultz, F., Kustka, A.B., Capone, D.G., 2011. Interbasin isotopic correspondence between upper-ocean bulk DON and subsurface nitrate and its implications for marine nitrogen cycling. *Global Biogeochem. Cycles* 25, GB4004. <http://dx.doi.org/10.1029/2010GB003878>.
- Knapp, A.N., Sigman, D.M., Kustka, A.B., Sañudo-Wilhelmy, S.A., Capone, D.G., 2012. The distinct nitrogen isotopic compositions of low and high molecular weight marine DON. *Mar. Chem.* 136–137, 24–33.
- Knicker, H., Hatcher, P.G., 2001. Sequestration of organic nitrogen in the sapropel from Mangrove Lake, Bermuda. *Org. Geochem.* 32, 733–744.
- Landolfi, A., Oschlies, A., Sanders, R., 2008. Organic nutrients and excess nitrogen in the North Atlantic subtropical gyre. *Biogeosciences* 5 (5), 1199–1213. <http://dx.doi.org/10.5194/bg-5-1199-2008>.
- Lee, C., Bada, J.L., 1977. Dissolved Amino Acids in the Equatorial Pacific, the Sargasso Sea, and Biscayne Bay. *Limnol. Oceanogr.* 22 (3), 502–510.
- Lee, S., Fuhrman, J.A., 1997. Relationships between biovolume and biomass of naturally derived marine bacterioplankton. *Appl. Environ. Microbiol.* 53, 1298–1303.
- Lehman, J. 2009. Compound specific amino acid isotopes as tracers of algal central metabolism: developing new tools for tracing prokaryotic vs. eukaryotic primary production and organic nitrogen in the ocean. Master Thesis. University of California Santa Cruz.
- Liardon, R., Ledermann, S., Ott, U., 1981. Determination of D-amino acids by deuterium labeling and selected ion monitoring. *J. Chromatogr.* 203, 385–395.
- Macko, S.A., Fogel, M.L., Engel, M.H., Hare, P.E., 1986. Kinetic fractionation of stable nitrogen isotopes during amino acid transamination. *Geochim. Cosmochim. Acta* 50 (10), 2143–2146.
- Macko, S.A., Fogel, M.L., Hare, P.E., Hoering, T.C., 1987. Isotopic fractionation of nitrogen and carbon in the synthesis of amino acids by microorganisms. *Chem. Geol.* 65, 79–92.
- McCarthy, M.D., Bronk, D.A., 2008. Analytical methods for the study of nitrogen. In: Capone, D.G., Bronk, D.A., Mulholland, M.R., Carpenter, E.J. (Eds.), *Nitrogen in the Marine Environment*. Academic Press, Amsterdam, pp. 1219–1276.
- McCarthy, M.D., Hedges, J.L., Benner, R., 1996. Major biochemical composition of dissolved high molecular weight organic matter in seawater. *Mar. Chem.* 55, 281–297. [http://dx.doi.org/10.1016/S0304-4203\(96\)00041-2](http://dx.doi.org/10.1016/S0304-4203(96)00041-2).
- McCarthy, M.D., Pratum, T., Hedges, J.L., Benner, R., 1997. Chemical composition of dissolved organic nitrogen in the ocean. *Nature* 390, 150–154. <http://dx.doi.org/10.1038/36535>.
- McCarthy, M.D., Hedges, J.L., Benner, R., 1998. Major bacterial contribution to marine dissolved organic nitrogen. *Science* 281, 231–234. <http://dx.doi.org/10.1126/science.281.5374.231>.
- McCarthy, M.D., Benner, R., Lee, C., Hedges, J.L., Fogel, M., 2004. Amino acid carbon isotopic fractionation patterns in oceanic dissolved organic matter: an unaltered photoautotrophic source for dissolved organic nitrogen in the ocean? *Mar. Chem.* 92, 123–134.
- McCarthy, M.D., Benner, R., Lee, C., Fogel, M.L., 2007. Amino acid isotopic fractionation patterns as indicators of heterotrophy in plankton, particulate, and dissolved organic matter. *Geochim. Cosmochim. Acta* 71, 4727–4744. <http://dx.doi.org/10.1016/j.gca.2007.06.061>.
- McClelland, J.W., Montoya, J.P., 2002. Trophic relationships and the nitrogen isotopic composition of amino acids. *Ecology* 83, 2173–2180.
- McClelland, J.W., Holl, C.W., Montoya, J.P., 2003. Relating low $\delta^{15}\text{N}$ values of zooplankton to N_2 fixation in the tropical North Atlantic: insights provided by stable isotope ratios of amino acids. *Deep Sea Res.* 50, 849–861.
- Meador, T.B., Aluwihare, L.I., Mahaffey, C., 2007. Isotopic heterogeneity and cycling of organic nitrogen in the oligotrophic ocean. *Limnol. Oceanogr.* 52, 934–947. <http://dx.doi.org/10.4319/lo.2007.52.3.0934>.
- Mou, X.Z., Sun, S.L., Edwards, R.A., Hodson, R.E., Moran, M.A., 2008. Bacterial carbon processing by generalist species in the coastal ocean. *Nature* 451, 708–711.
- Nagata, T., 2000. Production mechanisms of dissolved organic matter. In: Kirchman, D.L. (Ed.), *Microbial Ecology of the Oceans*. John Wiley, New York, pp. 121–152.
- Osagawa, H., Amagai, Y., Koike, I., Kaiser, K., Benner, R., 2001. Production of refractory dissolved organic matter by bacteria. *Science* 292, 917–920.
- Pérez, M.T., Pausz, C., Herndl, G.J., 2003. Major shift in bacterioplankton utilization of enantiomeric waters and the ocean's interior. *Limnol. Oceanogr.* 48 (2), 755–763.
- Pomeroy, L.R., 1974. The ocean's food web, a changing paradigm. *Bioscience* 24, 499–504.
- Popp, B.N., Graham, B.S., Olson, R.J., Hannides, C., Lott, M.J., López-Ibarra, G.A., Galván-Magaña, F., Fry, B., 2007. Insight into the trophic ecology of yellowfin tuna, *Thunnus albacares*, from compound-specific nitrogen isotope analysis of proteinaceous amino acids. In: Dawson, T., Siegwolf, R. (Eds.), *Stable Isotopes as Indicators of Ecological Change*. Terrestrial Ecology Series. Elsevier Academic Press, pp. 173–190.
- Riebesell, U., Schulz, K.G., Bellerby, R.G., Botros, M., Fritsche, P., Meyerhöfer, M., Neill, C., Nondal, G., Oschlies, A., Wohlers, J., Zöllner, E., 2007. Enhanced biological carbon consumption in a high CO_2 ocean. *Nature* 450, 545–548.
- Roland, L.A., McCarthy, M.D., Peterson, T.D., Walker, B.D., 2008. A large-volume microfiltration system for isolating suspended particulate organic matter: fabrication and assessment versus GFF filters in central North Pacific. *Limnol. Oceanogr. Methods* 6, 64–80.
- Sharp, J.H., Carlson, C.A., Peltzer, E.T., Castle-Ward, D.M., Savidge, K.B., Rinker, K.R., 2002. Final dissolved organic carbon broad community intercalibration and preliminary use of DOC reference materials. *Mar. Chem.* 77, 239–253.
- Sherwood, O.A., Lehmann, M.F., Schubert, C.J., Scott, D.B., McCarthy, M.D., 2011. Nutrient regime shift in the western North Atlantic indicated by compound-specific $\delta^{15}\text{N}$ of deep-sea gorgonian corals. *Proceedings of the National Academy of Sciences*. <http://dx.doi.org/10.1073/pnas.1004904108>.
- Shleifer, K.H., Kandler, O., 1972. Peptidoglycan types of bacterial cell walls and their taxonomic implications. *Bacteriol. Rev.* 36, 407–477.
- Silfer, J.A., Engel, M.H., Macko, S.A., Jumeau, E.J., 1991. Stable carbon isotope analysis of amino acid enantiomers by conventional isotope ratio mass spectrometry and combined gas chromatography/isotope ratio mass spectrometry. *Anal. Chem.* 63, 370–374.
- Solórzano, L., 1969. Determination of ammonia in natural waters by the phenylhypochlorite method. *Limnol. Oceanogr.* 14, 799–801.
- Somes, C.J., Schmittner, A., Galbraith, E.D., Lehmann, M.F., Altabet, M.A., Montoya, J.P., Letelier, R.M., Mix, A.C., Bourbonnais, A., Eby, M., 2010. Simulating the global distribution of nitrogen isotopes in the ocean. *Global Biogeochem. Cycles* 24, GB4019. <http://dx.doi.org/10.1029/2009GB003767>.
- Suttle, C.A., 2007. Marine viruses — major players in the global ecosystem. *Nat. Rev. Microbiol.* 5, 801–812.
- Suttle, C.A., Chan, A.M., Cottrell, M.T., 1990. Infection of viruses by phytoplankton and reduction of primary productivity. *Nature* 347, 467–469.

- Vallino, J.J., Hopkinson, C.S., Hobbie, J.E., 1996. Modeling bacterial utilization of dissolved organic matter: optimization replaces Monod growth kinetics. *Limnol. Oceanogr.* 41, 1591–1609.
- Vranova, V., Zahradnickova, H., Janous, D., Skene, K.R., Matharu, A.S., Rejsek, K., Formanek, P., 2012. The significance of D-amino acids in soil, fate and utilization by microbes and plants: review and identification of knowledge gaps. *Plant Soil* 354, 21–39. <http://dx.doi.org/10.1007/s11104-011-1059-5>.
- Wakeham, S.G., Lee, C., Hedges, J.I., Hernes, P.J., Peterson, M.L., 1997. Molecular indicators of diagenetic status in marine organic matter. *Geochim. Cosmochim. Acta* 61, 5363–5369.
- Walker, B.D., Beaupre, S.R., Guilderson, T.P., Druffel, E.R.M., McCarthy, M.D., 2011. Large volume ultrafiltration for the study of radiocarbon signatures and size vs. age relationships in marine dissolved organic matter. *Geochim. Cosmochim. Acta* 75, 5187–5202.
- Williams, P.J.B., 1995. Evidence for the seasonal accumulation of carbon-rich dissolved organic material, its scale in comparison with changes in particulate material and the consequential effect on net C/N assimilation ratios. *Mar. Chem.* 51 (1), 17–29.
- Wonga, C.S., Yub, Z., Waserc, N.A.D., Whitneya, F.A., Johnsona, W.K., 2002. Seasonal changes in the distribution of dissolved organic nitrogen in coastal and open-ocean waters in the North East Pacific: sources and sinks. *Deep Sea Res. Part II* 49 (24–25), 5759–5773. [http://dx.doi.org/10.1016/S0967-0645\(02\)00213-8](http://dx.doi.org/10.1016/S0967-0645(02)00213-8).
- Yamashita, Y., Tanoue, E., 2003. Distribution and alteration of amino acids in bulk DOM along a transect from bay to oceanic waters. *Mar. Chem.* 82, 145–160.
- Ziegler, S., Fogel, M.L., 2003. Seasonal and diel relationships between the isotopic compositions of dissolved and particulate organic matter in freshwater ecosystems. *Biogeochemistry* 64, 25–52.